EPR spectra in all crystal orientations shows that there is a significant amount of interchain spin diffusion. This suggests that next-nearest-neighbor intrachain-exchange coupling is not the only contribution to zJ'.

The single-crystal EPR spectra and the crystal structure were obtained at room temperature, and the magnetic results were determined from data in the temperature region 5.0–60 K. Temperature-dependent interchain-exchange-coupling constants and crystal structure parameters have been observed,[5,24] and such phenomena could possibly be present in [Cu(dien)OAc](ClO$_4$). If this is true, contributions to the unusual behavior of the EPR spectra could arise from these effects. Low-temperature (<40K) single-crystal EPR spectra would be especially valuable for this complex. These measurements will be undertaken when the necessary equipment becomes available to us.

Acknowledgment. This work was supported in part by the National Science Foundation through Grant CHE 860 1438.

Registry No. [Cu(dien)OAc](ClO$_4$), 21279-30-1.

Supplementary Material Available: Listings of hydrogen atom positional parameters, anisotropic thermal parameters, and bond distances and bond angles in the diethylenetriamine ligand, the acetate ligand, and the perchlorate anion (4 pages); a listing of observed and calculated structure factors (8 pages). Ordering information is given on any current masthead page.

Contribution from the Laboratoire de Spectrochimie des Elêments de Transition, UA No. 420, Universitê de Paris-Sud, 91405 Orsay, France

Irregular Spin State Structure in Trinuclear Species: Magnetic and EPR Properties of $Mn^{II}Cu^{II}Mn^{II}$ and $Ni^{II}Cu^{II}Ni^{II}$ Compounds

Yu Pei, Yves Journaux, and Olivier Kahn*

Received July 16, 1987

In a dinuclear system AB where A and B are magnetic ions with local spins S_A and S_B, the spin multiplicity of the low-lying states monotonically varies versus the energy. The spin state structure is said to be regular. The $\chi_M T$ versus T plot (χ_M = molar magnetic susceptibility; T = temperature) continuously decreases or increases upon cooling down according to whether the interaction is antiferro- or ferromagnetic. In a linear trinuclear system ABA, the spin state structure is regular if $2S_A \leq S_B$ but otherwise becomes irregular. The spin multiplicity does not vary monotonically versus the energy anymore. When the A–B interaction is antiferromagnetic [$H = -J(S_{A1} \cdot S_B + S_{A2} \cdot S_B)$; $J < 0$], the ground state does not have the lowest spin if $2S_A > S_B + {}^1/_2$. This may lead to characteristic magnetic behavior with a minimum in the $\chi_M T$ versus T plot. Below the temperature of the minimum, the compound exhibits a ferromagnetic-like behavior. This behavior has been observed in two compounds, namely {Mn(Me$_6$-[14]-ane-N$_4$)]$_2$Cu(pba)}(CF$_3$SO$_3$)$_2$·2H$_2$O (**1**) and {[Ni(Me$_6$-[14]ane-N$_4$)]$_2$Cu(pba)}(ClO$_4$)$_2$ (**2**) with Me$_6$-[14]ane-N$_4$ = (±)-5,7,7,12,14,14-hexamethyl-1,4,8,11-tetraazacyclotetradecane and pba = propane-1,3-diylbis(oxamato). The magnetic properties of **1** and **2** have been quantitatively interpreted. **1**: $S = {}^9/_2$ ground state; $J = -36.6$ cm^{-1}. **2**: $S = {}^3/_2$ ground state with a zero-field splitting characterized by an axial parameter $|D| = 2.4$ cm^{-1}; $J = -124.5$ cm^{-1}. The X-band powder EPR spectrum of **1** shows the $\Delta M_S = \pm 1$ allowed transitions and the $\Delta M_S = \pm 2$ (and maybe also ± 3, ± 4) forbidden transitions within the $S = {}^9/_2$ state. The EPR spectrum of **2** at 5.8 K shows the transitions within the $\pm {}^1/_2$ Kramers doublet arising from the $S = {}^3/_2$ ground state. When the sample is warmed, a transition associated with the first excited doublet state appears.

Introduction

The field of molecular magnetism has known a rapid development in the last few years. It is perhaps not exaggerated to speak of a Renaissance of the field. It has already been emphasized that, among other reasons, this situation is due to the fact that this field lies at the meeting point of two apparently widely separated disciplines, namely molecular materials and bioinorganic chemistry.[1,2] As far as the field of molecular materials is concerned, one of the main challenges is the design of molecular ferromagnets. So far, several approaches have been proposed along this line,[3-5] and very recently the first genuine molecular systems ordering ferromagnetically have been reported.[6,7] One of the approaches consists first of synthesizing molecular entities with a large spin in the ground state and then of assembling them within the crystal lattice in a ferromagnetic fashion.[8-11] Recently, Iwamura et al. described polycarbene type molecules with a nonet ground state[8-10] and stressed that any other molecular system with such a high-spin multiplicity in the ground state did not exist so far. This result arises from the fact that eight electrons occupy eight quasi-degenerate molecular orbitals. Other strategies have been proposed to favor ferromagnetic interactions within a molecular entity, one of them being the orthogonality of the magnetic orbitals.[12] All require symmetry conditions that are often difficult to achieve. This is why we have decided to explore an alternative strategy allowing us to "throw off the yoke" of the symmetry requirements as much as possible, nevertheless leading to new molecular systems with a large spin in the ground state. This strategy is based on the concept of irregular spin state structure.

In the next section, we introduce the idea of spin state structure and the relation between the spin state structure and the magnetic behavior in the simple case of a dinuclear system; then we approach the case of a symmetrical trinuclear species, and we show that the spin state structure may be regular or irregular. In this latter

(1) See: *Magneto-structural Correlations in Exchange Coupled Systems*; Willett, R. D., Gatteschi, D., Kahn, O., Eds.; Nato ASI Series; Reidel: Dordrecht, The Netherlands, 1985; Series C, Vol. 140.
(2) Morgenstern-Badarau, I.; Cocco, D.; Desideri, A.; Rotilio, G.; Jordanov, J.; Duprê, N. *J. Am. Chem. Soc.* **1986**, *108*, 300.
(3) Kahn, O. *Angew. Chem., Int. Ed. Engl.* **1985**, *24*, 834 and references therein.
(4) Cairns, C. J.; Busch, D. H. *Coord. Chem. Rev.* **1986**, *69*, 1 and references therein.
(5) Breslow, R. *Pure Appl. Chem.* **1982**, *54*, 927.
(6) Pei, Y.; Verdaguer, M.; Kahn, O.; Sletten, J.; Renard, J. P. *J. Am. Chem. Soc.* **1986**, *108*, 7428.
(7) Miller, J.; Calabrese, J. C.; Epstein, A. J.; Bigelow, R. W.; Zhang, J. H. *J. Chem. Soc., Chem. Commun.* **1986**, 1026.
(8) Iwamura, H.; Sugawara, T.; Itoh, K.; Takui, T. *Mol. Cryst. Liq. Cryst.* **1985**, *125*, 251.
(9) Sagawura, T.; Bandow, S.; Kimura, K.; Iwamura, H.; Itoh, K. *J. Am. Chem. Soc.* **1986**, *108*, 368.
(10) Teki, Y.; Takui, T.; Itoh, K.; Iwamura, H.; Kobayashi, K. *J. Am. Chem. Soc.* **1986**, *108*, 2147.
(11) Pei, Y.; Kahn, O.; Sletten, J. *J. Am. Chem. Soc.* **1986**, *108*, 3143.
(12) Kahn, O.; Galy, J.; Journaux, Y.; Jaud, J.; Morgenstern-Badarau, I. *J. Am. Chem. Soc.* **1982**, *104*, 2165.

0020-1669/88/1327-0399$01.50/0

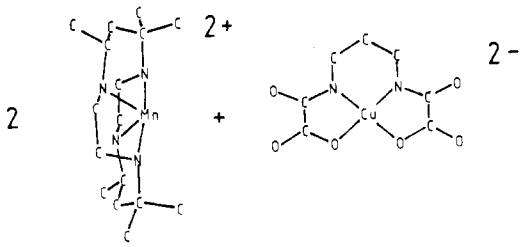

$$[(Mn[Me_6[14]aneN_4])_2Cu(pba)]^{2+}$$

Figure 1. Scheme showing the synthesis of **1**.

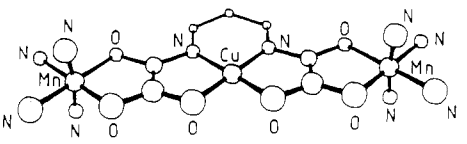

Figure 2. The $Mn^{II}Cu^{II}Mn^{II}$ trinuclear unit in **1**.

case, a ferromagnetic-like behavior can be obtained, with a ground state characterized by a large spin, even if the interaction between nearest-neighbor ions is antiferromagnetic. These ideas are applied to two trinuclear species, namely $\{[Mn(Me_6\text{-}[14]ane\text{-}N_4]_2Cu(pba)\}(CF_3SO_3)_2\cdot 2H_2O$ (**1**) and $\{[Ni(Me_6\text{-}[14]ane\text{-}N_4)]_2Cu(pba)\}(ClO_4)_2$ (**2**), also abbreviated hereafter as MnCuMn and NiCuNi, respectively. Me_6-[14]ane-N_4 is (±)-5,7,7,12,14,14-hexamethyl-1,4,8,11-tetraazacyclotetradecane[13] and pba is propane-1,3-diylbis(oxamato).[14] **1** and **2** are synthesized according to the scheme of Figure 1. The skeleton of **1** is shown in Figure 2. The magnetic and EPR properties of **1** and **2** are presented and interpreted quantitatively. Finally, the possibilities of this strategy in the framework of the synthesis of molecular ferromagnets are discussed. A preliminary communication of this work has already been published.[15]

Spin State Structure and Magnetic Behavior in Dinuclear Species

The interaction between two magnetic ions without orbital momentum at the first order, A and B, within a dinuclear compound leads to low-lying states, of which the relative energies are given by

$$E_S = -(J/2)S(S+1) \tag{1}$$

S denotes the spin of a given state and varies by an integer value from $|S_A - S_B|$ to $S_A + S_B$. S_A and S_B are the local spins of the interacting ions. J is the interaction parameter of the phenomenological Hamiltonian

$$\mathcal{H} = -J\hat{S}_A\cdot\hat{S}_B \tag{2}$$

J is negative or positive according to whether the interaction is antiferro- or ferromagnetic. For whatever the sign of J may be and for any values of S_A and S_B, the spin S varies monotonically versus the energy of the states. The system is said to present a *regular spin state structure*. This regularity leads to a simple correspondence between the nature of the interaction and the shape of the $\chi_M T$ versus T plot, χ_M being the molar magnetic susceptibility and T the temperature.

The high-temperature limit of $\chi_M T$, for $kT \gg |J|$, is the sum of what is expected for each of the isolated ions, i.e.

$$(\chi_M T)_{HT} = (N\beta^2/3k)[g_A^2 S_A(S_A+1) + g_B^2 S_B(S_B+1)] \tag{3}$$

where g_A and g_B denote the average values of the local g factors. In the absence of interaction ($J = 0$), $\chi_M T$ remains constant in the whole temperature range with the value given in (3); this is the Curie law. If the interaction is antiferromagnetic ($J < 0$), the ground state has the smallest spin $|S_A - S_B|$ and the most excited state the largest spin $S_A + S_B$. $\chi_M T$ continuously decreases upon cooling and tends toward the low-temperature limit

$$(\chi_M T)_{LT} = (N\beta^2 g_S^2/3k)[(S_A - S_B)^2 + |S_A - S_B|] \tag{4}$$

where g_S ($S = |S_A - S_B|$) is related to g_A and g_B by[16,17]

$$g_S = \frac{1+c}{2}g_A + \frac{1-c}{2}g_B \tag{5}$$

$$c = \frac{S_A(S_A+1) - S_B(S_B+1)}{S(S+1)} \tag{6}$$

In the particular case where S_A and S_B are equal, the ground state is diamagnetic and the χ_M versus T plot exhibits a characteristic maximum. If the interaction is ferromagnetic, the spectrum of the low-lying states is reversed. $\chi_M T$ continuously increases upon cooling and tends toward the low-temperature limit

$$(\chi_M T)_{LT} = (N\beta^2 g_S^2/3k)[(S_A + S_B)(S_A + S_B + 1)] \tag{7}$$

where g_S ($S = S_A + S_B$) is again related to g_A and g_B by (5) and (6).

In fact, the situation is slightly more complicated owing to the eventual zero-field splitting of the states with $S > 1/2$. In the following, we assume that this effect is small with regard to the isotropic interaction ($|D| \ll |J|$). Therefore, only the zero-field splitting within the ground state has an influence on the magnetic behavior.[18] Instead of exhibiting a plateau in the temperature range where only the ground state is thermally populated, the $\chi_M T$ versus T plot upon cooling to the low temperatures may tend to a value inferior to the limit given in (4) or (7). Neglecting this zero-field splitting effect, we can define a decrease of $\chi_M T$ upon cooling as an antiferromagnetic-like behavior and an increase of $\chi_M T$ as a ferromagnetic-like behavior. From the very large number of studies devoted to dinuclear magnetic systems, the fact clearly emerges that in most of the cases the interaction is antiferromagnetic. A brief survey of the literature published during the last decade indicates that less than 5% of the dinuclear compounds are ferromagnetically coupled.

Spin State Structure and Magnetic Behavior in Trinuclear Species

The concept of spin state structure is obviously not limited to dinuclear compounds; it is actually valid for any polymetallic species. However, when there are more than two interacting centers, a novel and very interesting situation appears; the spin state structure is not necessarily regular anymore, which can lead to quite original magnetic behaviors. We propose to develop this idea in the relatively simple case of a linear and symmetrical trinuclear species ABA. The local spins are again noted S_A and S_B. The interaction parameter in zero field may be written

$$\mathcal{H} = -J(\hat{S}_{A1}\cdot\hat{S}_B + \hat{S}_{A2}\cdot\hat{S}_B) \tag{8}$$

with $S_{A1} = S_{A2}$. In (8), it is assumed that the interaction between nearest neighbors is purely isotropic and that between terminal centers is negligible. The relative energies of the low-lying states are easily calculated as[19]

$$E_{S,S'} = -(J/2)[S(S+1) - S'(S'+1)] \tag{9}$$

S denotes the spin of a given state, and S', the spin associated with the terminal ions ($\hat{S}' = \hat{S}_{A1} + \hat{S}_{A2}$). In (9), S' varies by an integer value from 0 to $2S_A$ and for each S' value, S varies by

(13) Tait, A. M.; Busch, D. H. *Inorg. Nucl. Chem. Lett.* **1972**, *8*, 491.
(14) Monoyama, K.; Ojima, H.; Monoyama, M. *Inorg. Chim. Acta* **1976**, *20*, 127.
(15) Pei, Y.; Journaux, Y.; Kahn, O.; Dei, A.; Gatteschi, D. *J. Chem. Soc., Chem. Commun.* **1986**, 1300.
(16) Chao, C. C. *J. Magn. Reson.* **1973**, *10*, 1.
(17) Scaringe, R. P.; Hodgson, D.; Hatfield, W. E. *Mol. Phys.* **1978**, *35*, 701.
(18) Journaux, Y.; Kahn, O.; Zarembowitch, J.; Galy, J.; Jaud, J. *J. Am. Chem. Soc.* **1983**, *105*, 7585.
(19) Kambe, K. *J. Phys. Soc. Jpn.* **1950**, *5*, 48.

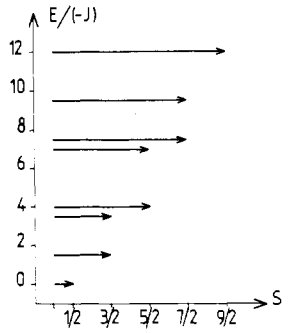

Figure 3. Spin state structure for an ABA trinuclear species with S_A = 1 and $S_B = {}^5/_2$.

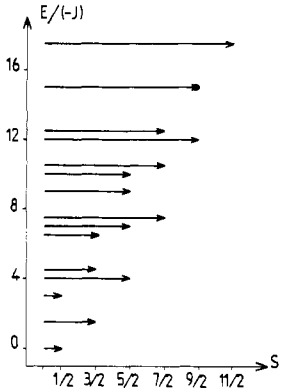

Figure 4. Spin state structure for an ABA trinuclear species with $S_A = {}^3/_2$ and $S_B = {}^5/_2$.

an integer value from $|S' - S_B|$ to $S' + S_B$. Three situations, as follows, may be distinguished concerning the distribution in energy of the spin states, according to the relative values of S_A and S_B.

(i) If $2S_A \leq S_B$, the spin state structure is regular. In the case of antiferromagnetic interaction ($J < 0$), the ground state has the smallest spin $S_B - 2S_A$ and the most excited state the highest spin $S_B + 2S_A$. For two states with the energies $E_1 < E_2$, one always has the spins $S_1 \leq S_2$.[20] $\chi_M T$ decreases in a continuous fashion when T decreases. In the case of ferromagnetic interaction ($J > 0$), the spectrum of the low-lying states is reversed and $\chi_M T$ continuously increases when T decreases.

Several trinuclear compounds with a regular spin state structure have been described. All present an antiferromagnetic interaction between nearest neighbors,[21-25] but two $Cu^{II}Gd^{III}Cu^{II}$ complexes.[26,27] To illustrate the concept of regular spin state structure in a trinuclear species ABA, we schematized the spin state structure for $S_A = 1$ and $S_B = {}^5/_2$ in Figure 3. Each state is represented by an arrow of which the length is equal to the spin associated with this state.

(ii) If $2S_A = S_B + {}^1/_2$ with S_A and $S_B \neq {}^1/_2$, the spin state structure becomes irregular. For $J < 0$, one may have $E_1 < E_2$ with $S_1 > S_2$. However, the ground state is a doublet and retains the lowest spin multiplicity. The calculation shows that again $\chi_M T$ continuously decreases upon cooling. An example of such an intermediate case is provided by $S_A = {}^3/_2$ and $S_B = {}^5/_2$. The spin state structure is shown in Figure 4.

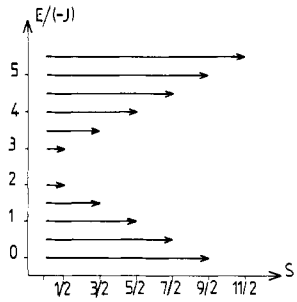

Figure 5. Spin state structure for an ABA trinuclear species with $S_A = {}^5/_2$ and $S_B = {}^1/_2$ ($Mn^{II}Cu^{II}Mn^{II}$).

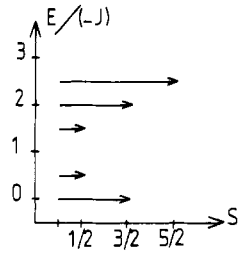

Figure 6. Spin state structure for an ABA trinuclear species with S_A = 1 and $S_B = {}^1/_2$ ($Ni^{II}Cu^{II}Ni^{II}$).

(iii) Finally, if $2S_A > S_B + {}^1/_2$, the spin state structure is even more irregular, and for $J < 0$, the spin $2S_A - S_B$ of the ground state is not the smallest spin anymore. On the other hand, the most excited state is again that with the largest spin $2S_A + S_B$. To discuss this problem, we consider the specific case $S_A = {}^5/_2$ and $S_B = {}^1/_2$ corresponding to a $Mn^{II}Cu^{II}Mn^{II}$ species. The spin state structure is shown in Figure 5. For $J < 0$, which is by far the most likely, the ground state is $S = {}^9/_2$. Upon an increase in energy above the ground state, the spin regularly decreases from ${}^9/_2$ to ${}^1/_2$ and then increases from ${}^1/_2$ to ${}^{11}/_2$ for the most excited state. It turns out that the low-energy range of the spin state structure is reminiscent of a ferromagnetically coupled system, in the sense where the lower the energy is, the higher the spin multiplicity. On the other hand, the high-energy range ($E > -5J/2$) corresponds well to what is implicitly expected for an antiferromagnetically coupled system. The high-temperature limit ($kT \gg |J|$) of $\chi_M T$ for such a ${}^5/_2$, ${}^1/_2$, ${}^5/_2$ system is equal to the sum of the contributions of the isolated ions:

$$\chi_M T = (n\beta^2/12k)(70g_A^2 + 3g_B^2) \simeq 9.1 \text{ cm}^3 \text{ mol}^{-1} \text{ K} \quad (10)$$

Upon cooling, the first state to be depopulated is that of the largest spin $S = {}^{11}/_2$, so that $\chi_M T$ decreases. In the low-temperature range now, when T decreases, one progressively depopulates states of low spin in favor of states of higher spin so that $\chi_M T$ is expected to increase up to a plateau in the temperature range where only the ground $S = {}^9/_2$ state is thermally populated, with

$$\chi_M T = 33N\beta^2 g_{9/2,5}{}^2/4k \simeq 12.4 \text{ cm}^3 \text{ mol}^{-1} \text{ K} \quad (11)$$

$g_{9/2,5}$ being the Zeeman factor associated with the ground state (vide infra). In summary, the $\chi_M T$ versus T plot is expected to exhibit a minimum and in the temperature range below this miminium to increase in a ferromagnetic-like fashion. The more pronounced the antiferomagnetic interaction is, the higher the temperature of the minimum of $\chi_M T$ and the broader the temperature range where $\chi_M T$ varies in a ferromagnetic-like fashion. To our knowledge, such magnetic behavior with a miminum in the $\chi_M T$ versus T plot has been mentioned for the fist time, without being discussed, by Ginsberg et al. for nickel(II) trimers.[28] Qualitatively, a similar situation is expected for a $S_A = 1$, $S_B = {}^1/_2$ antiferromagnetically coupled system such as $Ni^{II}Cu^{II}Ni^{II}$. The appropriate spin state structure is shown in Figure 6, with a ${}^3/_2$ ground state and just above two ${}^1/_2$ states, then a ${}^3/_2$ state, and

(20) For $S_A = 1$ and $S_B = 2$, one can have $E_1 = E_2$ and $S_1 < S_2$, which is not in contradiction with the statement that $E_1 < E_2$ imposes $S_1 \leq S_2$.
(21) Gruber, S. J.; Harris, C. M.; Sinn, E. *J. Chem. Phys.* **1968**, *49*, 2183; *J. Inorg. Nucl. Chem.* **1968**, *30*, 1805.
(22) Sinn, E. In *Biological and Inorganic Copper Chemistry*; Karlin, K. D., Zubieta, J., Eds.; Adenine: Guilderland, NY; 1985; Vol. 2, p 195.
(23) Morgenstern-Badarau, I.; Wickman, H. H. *Inorg. Chem.* **1985**, *24*, 1889.
(24) Sekutowski, D.; Jungst, R.; Stucky, G. D. *Inorg. Chem.* **1978**, *17*, 1848.
(25) Journaux, Y.; Sletten, J.; Kahn, O. *Inorg. Chem.* **1986**, *25*, 439.
(26) Bencini, A.; Benelli, C.; Caneschi, A.; Carlin, R. L.; Dei, A.; Gatteschi, D. *J. Am. Chem. Soc.* **1985**, *107*, 8128.
(27) Bencini, A.; Benelli, C.; Caneschi, A.; Dei, A.; Gatteschi, D. *Inorg. Chem.* **1986**, *25*, 572.
(28) Ginsberg, A. P.; Martin, R. L.; Sherwood, R. C. *Inorg. Chem.* **1968**, *7*, 932.

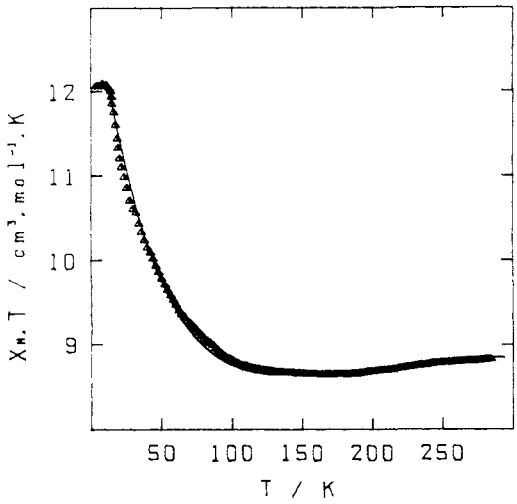

Figure 7. Experimental (△) and calculated (—) temperature dependences of $\chi_M T$ for **1**.

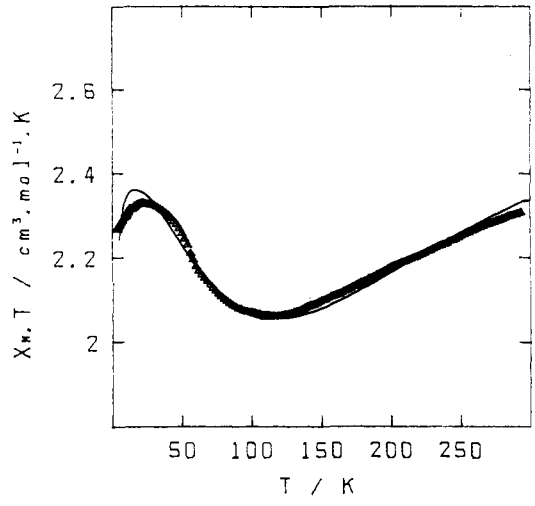

Figure 8. Experimental (△) and calculated (—) temperature dependences of $\chi_M T$ for **2**.

finally a $^5/_2$ state. Whatever S_A and S_B may be, when $J > 0$, there is no "anomally" in the magnetic behavior and $\chi_M T$ continuously increases when T decreases.

The ideas presented above concerning the irregular spin state structures will be applied to the understanding of the magnetic and EPR properties of compounds **1** and **2** in the next two sections.

Magnetic Properties

MnCuMn (1). The $\chi_M T$ versus T plot for **1** is shown in Figure 7. At room temperature, $\chi_M T$ is equal to 8.83 cm^3 mol^{-1} K and very smoothly decreases upon cooling. $\chi_M T$ reaches the expected minimum around 170 K with $\chi_M T = 8.64$ cm^3 mol^{-1} K. Below 170 K, $\chi_M T$ rapidly increases and reaches a plateau in the 2–10 K temperature range with $\chi_M T = 12.1$ cm^3 mol^{-1} K. To fit the experimental data, we used the theoretical expression of the magnetic susceptibility deduced from the spin Hamiltonian

$$\mathcal{H} = -J(\hat{S}_{Mn1}\cdot\hat{S}_{Cu} + \hat{S}_{Mn2}\cdot\hat{S}_{Cu}) + \beta[g_{Mn}(\hat{S}_{Mn1} + \hat{S}_{Mn2}) + g_{Cu}\hat{S}_{Cu}]\cdot\vec{H} \quad (12)$$

This expression is

$$\chi_M = \frac{N\beta^2}{k(T-\Theta)}\left[\sum_{S'=0}^{2S_A}\sum_{S=|S'-S_B|}^{S'+S_B} g_{S,S'}^2 S(S+1)(2S+1)\times \exp\left(-\frac{E_{S,S'}}{kT}\right)\right] \Big/ \left[\sum_{S'=0}^{2S_A}\sum_{S=|S'-S_B|}^{S'+S_B}(2S+1)\exp\left(-\frac{E_{S,S'}}{kT}\right)\right] \quad (13)$$

A Weiss correction Θ has been introduced to account for eventual small intermolecular interactions. The $g_{S,S'}$ factors are related to g_A and g_B by[29]

$$g_{S,S'} = \{g_A[S(S+1) + S'(S'+1) - S_B(S_B+1)] + g_B[S(S+1) - S'(S'+1) + S_B(S_B+1)]\}/[2S(S+1)] \quad (14)$$

with $S_A = {}^5/_2$ and $S_B = {}^1/_2$. In (12) and (13), we neglected the local anisotropy of the Mn^{II} ions (see the EPR section) as well as the anisotropic interactions. Moreover, we assumed that the local g factors were isotropic. The minimization of $R = \sum|\chi_M T^{obsd} - \chi_M T^{calcd}|^2/\sum|\chi_M T^{obsd}|^2$ leads to $J = -36.6$ cm^{-1}, $g_{Mn} = 2.03$, $g_{Cu} = 2.10$, and $\Theta = -0.31$ K. R is then equal to 3.9×10^{-5} cm^{-1}.

In order to confirm the nature of the ground state, we estimated the saturation magnetization M_S by extrapolating the magnetization versus magnetic field curve measured in the range 10^4–5×10^4 G at 4.2 K and found $(49 \pm 2) \times 10^3$ cm^3 mol^{-1} G. The theoretical value $Ng\beta S$ with $g = 2$ and $S = {}^9/_2$ is calculated as 50.17×10^3 cm^3 mol^{-1} G. At 5×10^4 G and 4.2 K, the magnetization is equal to 46.7×10^3 cm^3 mol^{-1} G, i.e. 93% of M_S, whereas the Brillouin function for this H/T value is equal to 0.944.

NiCuNi (2). The $\chi_M T$ versus T plot for **2** is shown in Figure 8. At 290 K, $\chi_M T$ is equal to 2.31 cm^3 mol^{-1} K. It decreases upon cooling, reaches a minimum around 118 K with $\chi_M T = 2.06$ cm^3 mol^{-1} K, then increases to a rounded maximum about 21 K with $\chi_M T = 2.33$ cm^3 mol^{-1} K, and finally slightly decreases again upon cooling to 2 K. Since the EPR spectrum clearly shows a fine structure within the $S = {}^3/_2$ ground state (vide infra), the magnetic behavior of **2** below 22 K is attributed to the splitting in zero field of this ground state rather than to intermolecular interactions. To take into account this effect, we deduced the expression of the magnetic susceptibility from the spin Hamiltonian

$$\mathcal{H} = -J(\hat{S}_{Ni1}\cdot\hat{S}_{Cu} + \hat{S}_{Ni2}\cdot\hat{S}_{Cu}) + D[\hat{S}_z^2 - {}^1/_3 S(S+1)]\delta_{S,3/2}\delta_{S',2} + \beta[g_{Ni}(\hat{S}_{Ni1} + \hat{S}_{Ni2}) + g_{Cu}\hat{S}_{Cu}]\cdot\vec{H} \quad (15)$$

where the splitting within the ground state is assumed to be axial for the sake of simplicity. The EPR spectrum shows that in fact this splitting is rhombic. The parallel and perpendicular magnetic susceptibilities are then

$$\chi_\parallel = \frac{N\beta^2}{4kT}\left\{g_{3/2,2}^2\left[9\exp\left(-\frac{D}{kT}\right) + \exp\left(\frac{D}{kT}\right)\right] + g_{1/2,1}^2\exp\left(\frac{J}{2kT}\right) + g_{1/2,0}^2\exp\left(\frac{3J}{2kT}\right) + 10g_{3/2,1}^2\exp\left(\frac{2J}{kT}\right) + 35g_{5/2,2}^2\exp\left(\frac{5J}{2kT}\right)\right\} \Big/ \left\{\exp\left(-\frac{D}{kT}\right) + \exp\left(\frac{D}{kT}\right) + \exp\left(\frac{J}{2kT}\right) + \exp\left(\frac{3J}{2kT}\right) + 2\exp\left(\frac{2J}{kT}\right) + 3\exp\left(\frac{5J}{2kT}\right)\right\} \quad (16)$$

$$\chi_\perp = \frac{N\beta^2}{4kT}\left\{g_{3/2,2}^2\left[-\frac{3kT}{D}\exp\left(-\frac{D}{kT}\right) + \left(4 - \frac{3kT}{D}\right)\exp\left(\frac{D}{kT}\right)\right] + g_{1/2,1}^2\exp\left(\frac{J}{2kT}\right) + g_{1/2,0}^2\times \exp\left(\frac{3J}{2kT}\right) + 10g_{3/2,1}^2\exp\left(\frac{2J}{kT}\right) + 35g_{5/2,2}^2\exp\left(\frac{5J}{2kT}\right)\right\} \Big/ \left\{\exp\left(-\frac{D}{kT}\right) + \exp\left(\frac{D}{kT}\right) + \exp\left(\frac{J}{2kT}\right) + \exp\left(\frac{3J}{2kT}\right) + 2\exp\left(\frac{2J}{kT}\right) + 3\exp\left(\frac{5J}{2kT}\right)\right\} \quad (17)$$

In (15)–(17), it has been assumed that the local g factors were isotropic and that the spin states did not couple through the local anisotropy of the Ni^{II} ion ($|J| \gg D_{Ni}$).[30-32] The $g_{S,S'}$ factors have

(29) Journaux, Y. Ph.D. Thesis, Université de Paris-Sud, Orsay, France, 1985.

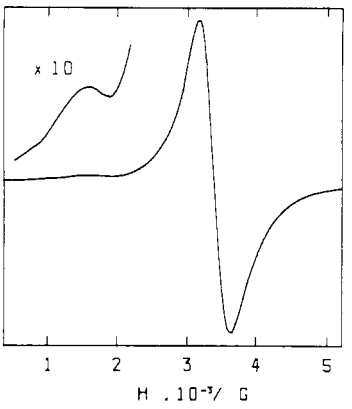

Figure 9. X-Band powder EPR spectrum of **1** at 4.2 K.

been related to g_{Ni} and g_{Cu} by (14), which is consistent with the approximation $|J| \gg D_{Ni}$.

The least-squares fitting of the experimental data leads to two equally satisfying solutions, according to whether D is positive or negative. These solutions are $J = -124.5$ cm^{-1}, $g_{Ni} = 2.24$, $g_{Cu} = 2.18$, and $D = \pm 2.4$ cm^{-1} with $R = 6.5 \times 10^{-5}$.

D is due to both the local anisotropy of the Ni^{II} ions and the anisotropic interaction. The zero-field-splitting tensor **D** within the $S = {}^3/_2$ ground state can be easily related to the local anisotropy tensors $\mathbf{D}_{Ni1}$ and $\mathbf{D}_{Ni2}$ and to the anisotropic interaction tensors $\mathbf{D}_{Ni1Cu}$ and $\mathbf{D}_{Ni2Cu}$ by

$$\mathbf{D} = \frac{7}{30}(\mathbf{D}_{Ni1} + \mathbf{D}_{Ni2}) - \frac{1}{10}(\mathbf{D}_{Ni1Cu} + \mathbf{D}_{Ni2Cu}) \qquad (18)$$

EPR Spectra

MnCuMn (1). The X-band powder EPR spectrum of **1** at 4.2 K is shown in Figure 9. It presents an intense feature at 3402 G ($g = 1.99$) and a well-resolved half-field signal at 1710 G ($g = 3.96$). When magnifying the spectrum, one can detect very weak signals around 1153 G ($g \simeq 5.88$) and 764 G ($g \simeq 8.87$). The spectrum also shows a shoulder at very low field, around 300 G.

The first two signals most likely correspond to the envelopes of the $\Delta M_S = \pm 1$ and ± 2 transitions, respectively, within the $S = {}^9/_2$ ground state. The aspect of the spectrum indicates that the fine structure for this ground state is weak, which is consistent with the magnetic data. In the frame of this interpretation, it is tempting to assign the weak signals at $g \simeq 5.88$ and 8.87 to the $\Delta M_S = \pm 3$ and ± 4 transitions, respectively. The origin of the low-field shoulder at 300 G remains unclear for us.

The appearance of the $\Delta M_S = \pm 2$, ± 3, and ± 4 forbidden transitions can be rather easily justified. In the present case, the fine structure may be treated as a perturbation with regard to the dominant Zeeman term

$$\mathcal{H}_{ZE} = g\beta(l\hat{S}_x + m\hat{S}_y + n\hat{S}_z)\cdot\vec{H} \qquad (19)$$

(19) can be transformed into

$$\mathcal{H}_{ZE} = g\beta\hat{S}'_z\cdot\vec{H} \qquad (20)$$

owing to the rotation of a φ angle defined as

$$\varphi = (g_x/g_z)\tan\theta \qquad (21)$$

where θ is the angle between H and the z axis. The fine structure term

$$D[S_z^2 - {}^1/_3 S(S+1)]$$

becomes in the new basis[33]

$$\mathcal{H}_{FS} = {}^1/_2 D[\hat{S}'^2_z - {}^1/_3 S(S+1)](3\cos^2\varphi - 1) - D(\hat{S}'_x\cdot\hat{S}'_z + \hat{S}'_z\cdot\hat{S}'_x)\cos\varphi\sin\varphi + {}^1/_4 D(\hat{S}_+^2 + \hat{S}_-^2)\sin^2\varphi \qquad (22)$$

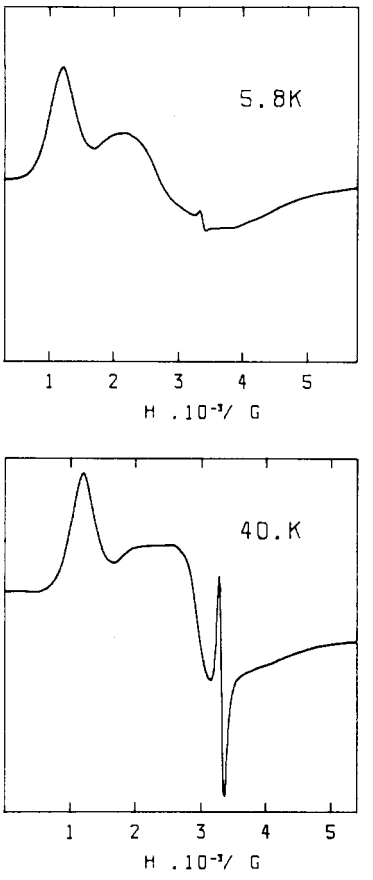

Figure 10. X-Band powder EPR spectra of **2** at 5.8 and 40 K.

and mixes any $|M_S\rangle$ ket with $|M_S \pm 1\rangle$ and $|M_S \pm 2\rangle$, which activates the forbidden transitions. This mixing occurs for any $\sin\varphi \neq 0$, i.e. when H is not parallel to the z axis. The ratio of the intensities $I(\Delta M_S = \pm 2)/I(\Delta M_S = \pm 1)$ is of the order of $(D/g\beta H)^2$; that of the intensities $I(\Delta M_S = \pm 3, \pm 4)/I(\Delta M_S = \pm 1)$, of the order of $(D/g\beta H)^4$.

NiCuNi (2). The spectra of **2** at 5.8 and 40 K are shown in Figure 10. The spectrum at 5.8 K presents four features: a resonance with a maximum at 1206 G ($g = 5.61$), a broad band centered around 2810 G ($g = 2.41$), a shoulder around 3700 G ($g = 1.83$), and a very weak signal centered at 3362 G ($g = 2.02$). Upon warming to 40 K, the relative intensity of the signal at $g = 2.02$ increases with regard to the other three features. In addition, a new transition around 3000 G ($g = 2.26$) appears, quenching partly the broad band at 2810 G. The qualitative interpretation of these spectra is relatively simple. The spectrum at 5.8 K is associated with the Kramers doublet $\pm {}^1/_2$ arising from the $S = {}^3/_2$ ground state. This spectrum presents, as expected, a strong rhombicity with $g_1 = 5.6$, $g_2 = 2.4$, and $g_3 = 1.8$. On this spectrum is superimposed that of the first doublet excited state, of which the intensity increases upon warming. The transition around 3000 G, which appears when the temperature increases, could be associated with the second doublet excited state.

The aspect of the spectrum at 5.8 K points out that we are in the case where the zero-field splitting within the quadruplet ground state is larger than the incident quantum ($|D| > h\nu$), which again is consistent with the interpretation of the magnetic data. The spectrum does not show any signal associated with the $\pm {}^3/_2$ Kramers doublet.

Discussion

In this work, we have shown that it was possible to synthesize a molecular system with a high-spin multiplicity in the ground state and ferromagnetic-like behavior in the low-temperature

(30) Bencini, A.; Gatteschi, D. *Mol. Phys.* **1985**, *54*, 969.
(31) Hulliger, J. Ph.D. Thesis, University of Zurich, Zurich, Switzerland, 1984.
(32) Journaux, Y.; Kahn, O.; Morgenstern-Badarau, I.; Galy, J.; Jaud, J.; Bencini, A.; Gatteschi, D. *J. Am. Chem. Soc.* **1985**, *107*, 6305.
(33) Abragam, A.; Bleaney, B. *Electron Paramagnetic Resonance of Transition Ions*; Clarendon: New York, 1970.

range, without imposing ferromagnetic interactions between nearest-neighbor ions. The basic idea is that of an irregular spin state structure, of which the MnCuMn compound **1** provides a spectacular example (see Figure 5). A vivid way to describe the ground state of **1** is to say that the two $^5/_2$ local spins on the terminal ions are aligned along a common direction through the antiferromagnetic interaction with the $^1/_2$ local spin of the copper(II) ion, according to

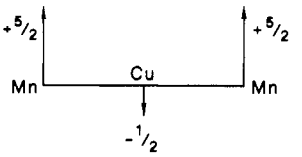

In some way, the small central spin polarizes the two large terminal spins in a ferromagnetic-like fashion. To our knowledge, the MnCuMn compound **1** is one of the molecular systems with the largest spin in the ground state. Moreover, this $S = {}^9/_2$ ground state is rather well separated in energy from the first excited state since the energy gap between those two states is found as $-J/2 = 18.3\ cm^{-1}$. Two other molecular systems with a $S = {}^9/_2$ ground state have recently been reported. Both are $Cu^{II}Gd^{III}Cu^{II}$ trinuclear complexes[26,27] in which the Cu–Gd interaction was claimed to be ferromagnetic. The interaction between a rare-earth element and any other magnetic ion, however, is very weak so that the ground state is much less isolated from the first excited state.

Concerning the compounds **1** and **2** described in this paper, it is quite important to stress that the stronger the Mn–Cu or the Ni–Cu antiferromagnetic interaction is, the broader the temperature range where $\chi_M T$ varies in a ferromagnetic-like fashion. Consequently, the choice of bis-bidentate bridging ligands such as oxamato was well adapted to our aim. Indeed, these bridges are known to favor strong antiferromagnetic interactions between metal ions, provided that on each ion there is a magnetic orbital of *xy* symmetry, schematized as follows:

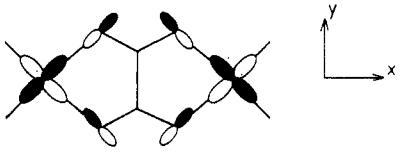

For Mn^{II} and Ni^{II} as well as Cu^{II}, such a magnetic orbital is available. In **1**, the minimum of $\chi_M T$ occurs at 170 K and in **2** at 118 K.

So far, we have proposed two strategies to design molecular systems with a large spin in the ground state; the former is that of strict orthogonality of the magnetic orbitals; the latter, that described in this paper. We want to point out that the former strategy, although leading to ferromagnetic interactions between nearest neighbors, is not more efficient than the latter one. For that, we again consider an ABA symmetrical trinuclear species where A and B are 3d metal ions (we exclude the rare-earth elements) and we look for the arrangement giving the largest spin. If we use the strategy of orthogonality, the answer is $Cr^{III}Ni^{II}Cr^{III}$. Indeed Cr^{III} in octahedral surroundings has three unpaired electrons in t_{2g} orbitals and Ni^{II} also in octahedral surroundings has two unpaired electrons in e_g orbitals. If the whole symmetry is high enough to retain the orthogonality of the t_{2g} and e_g orbitals ($\langle t_{2g}|e_g\rangle = 0$), the Cr–Ni interaction will be ferromagnetic and the $Cr^{III}Ni^{II}Cr^{III}$ unit will have a $S = 4$ ground state. This result is inferior to that obtained with $Mn^{II}Cu^{II}Mn^{II}$, for which the ground state is $S = {}^9/_2$.

The magnetic data for **1** and **2** have been investigated down to 2 K and no indication of long-range ordering has appeared, which is not surprising owing to the presence of bulky terminal ligands and counteranions. One of our goals, however, is to design molecular ferromagnets. This requires, of course, organization of the high-spin molecular units in the crystal lattice in a way to favor a parallel alignment of the molecular spins, and we are presently working along this line. One of the solutions, but not the only one, is to synthesize an $A_1 = Mn^{II}Cu^{II}Mn^{II}$ species with a $^9/_2$ spin, then an $A_2 = A_1Cu^{II}A_1$ species with a $^{17}/_2$ or a $^{19}/_2$ spin, and so on. Such a process may lead to the $Mn^{II}Cu^{II}$ ferrimagnetic chains that have already been described.[6,11,34,35] In one case, so far, we succeeded in organizing those chains in such a way that the compound presents a ferromagnetic transition.[6]

To conclude, we wish to emphasize that the conceptual approach utilized in this work can be extended to three-dimensional lattices and lead to novel systems exhibiting a ferromagnetic transition.

Experimental Section

Syntheses. MnCuMn (1). $[Mn(Me_6\text{-}[14]ane\text{-}N_4)](CF_3SO_3)_2$ was synthesized by following a procedure analogous to that reported for the meso derivative,[36] and $Na_2[Cu(pba)]\cdot 6H_2O$ was obtained as previously described.[14]

1 was obtained by adding a solution of 10^{-3} mol of $[Mn(Me_6\text{-}[14]ane\text{-}N_4)](CF_3SO_3)_2$ in a mixture of 50 mL of methanol and 10 mL of acetonitrile to a solution of 0.5×10^{-3} mol of $Na_2[Cu(pba)]\cdot 6H_2O$ in 20 mL of water. **1** precipitated as a brown microcrystalline powder.

Anal. Calcd for $C_{41}H_{82}N_{10}O_{14}F_6S_2CuMn_2$ (**1**): C, 38.15; H, 6.40; N, 10.85; S, 4.97; Cu, 4.92; Mn, 8.51. Found: C, 38.04; H, 5.91; N, 10.65; S, 4.95; Cu, 5.06; Mn, 8.65.

NiCuNi (2). $[Ni(Me_6\text{-}[14]ane\text{-}N_4)](ClO_4)_2$ was synthesized as previously described.[37] **2** was prepared as follows: 20 mL of an aqueous solution of 0.5×10^{-3} mol of $Na_2[Cu(pba)]\cdot 6H_2O$ was slowly added to a solution of 10^{-3} mol of $[Ni(Me_6\text{-}[14]ane\text{-}N_4](ClO_4)_2$ in a mixture of 40 mL of methanol and 20 mL of acetonitrile. Slow evaporation afforded small crystals of **2**.

Anal. Calcd for $C_{39}H_{78}N_{10}O_{14}Cl_2CuNi_2$ (**2**): C, 40.28; H, 6.76; N, 12.05; Cu, 5.46; Ni, 10.09. Found: C, 40.34; H, 6.83; N, 12.26; Cu, 5.18; Ni, 10.04.

Magnetic Measurements. These were carried out with a Faraday type magnetometer equipped with a He continuous-flow cryostat working in the 2–300 K temperature range. For both **1** and **2**, the independence of the susceptibility versus the applied field was checked at room temperature and 4.2 K. Mercury tetrakis(thiocyanato)cobaltate was used as a susceptibility standard. Diamagnetic corrections were estimated as -483×10^{-6} and $-443 \times 10^{-6}\ cm^3\ mol^{-1}$ for **1** and **2**, respectively.

Magnetization data in the 10^4–5×10^4 G magnetic field range were recorded with a laboratory-made apparatus working according to the extraction method.

EPR Spectra. These were recorded on powder samples at X-band frequency with a Bruker ER 200D spectrometer equipped with an Oxford Instruments continuous-flow cryostat. The magnetic field was determined with a Hall probe, and the Klystron frequency, with a Hewlett-Packard frequency meter.

Registry No. **1**, 106396-99-0; **2**, 111976-29-5.

(34) Gleizes, A.; Verdaguer, M. *J. Am. Chem. Soc.* **1984**, *106*, 3727.
(35) Kahn, O. *Struct. Bonding (Berlin)* **1987**, *68*, 89.
(36) Bryan, P. S.; Dabrowiak, J. C. *Inorg. Chem.* **1975**, *14*, 296.
(37) Curtis, N. F.; Swann, D. A.; Waters, T. N. *J. Chem. Soc., Dalton Trans.* **1973**, 1963.